Current-driven switching of topological spin chirality in a van der Waals antiferromagnet

Kai-Xuan Zhang,* Seungbok Lee, Woonghee Cho, and Je-Geun Park*

Department of Physics and Astronomy, Seoul National University, Seoul 08826, South Korea E-mail: kxzhang.research@gmail.com; jgpark10@snu.ac.kr

Keywords: Topological spin chirality, Intercalated van der Waals $Co_{1/3}TaS_2$, Electrical control, Switch spin chirality, Spin-orbit torque, Metallic quantum antiferromagnet.

Abstract: Magnetic topology is central to modern quantum magnet, where spin chirality governs exotic spin winding, real-space Berry phase, and topological Hall effect. A key unresolved challenge is how to electrically switch topological spin chirality and its associated gauge flux, an essential requirement for manipulating its topological quantum properties. In this work, we propose and experimentally demonstrate the concept of current-switching spin chirality. We identify the new vdW antiferromagnet Co_{1/3}TaS₂ as an ideal platform, hosting a topological 3Q state with a minimum chirality cell, an ultrahigh skyrmion density, a non-centrosymmetric geometry, and a strong Berry curvature. Using a Co_{1/3}TaS₂/Pt heterostructure, we achieve the nonvolatile and reversible switching by current via current-driven spin-orbit torque based on Pt's spin Hall effect. Beyond this conventional route, we further discover intrinsic self-torque-induced chirality switching within Co_{1/3}TaS₂, driven purely by current, without a magnetic field, and with high energy efficiency. These complementary pathways establish a unified framework for electrically creating and controlling spin chirality. Our results demonstrate a practical route toward

chiral spintronics. They can be naturally generalised to other skyrmion systems, offering new opportunities in symmetry control, topological manipulation, and spin-chirality-based quantum functionalities.

Main Text: Spin chirality naturally emerges in non-coplanar spin texture and represents one of the most intriguing quantum characteristics of magnetic topology^{1,2}. In the canonical three-spin model, the scalar spin chirality is defined as $\chi = \langle S_1 \cdot (S_2 \times S_3) \rangle$, where S_1 , S_2 , and S_3 denote spins located on a triangular plaquette^{1,2}. When an electron moves through such a topological spin configuration, it acquires a real-space Berry phase, giving rise to a variety of topological quantum phenomena, most notably the topological Hall effect^{1,2}. In this sense, spin chirality acts as an emergent magnetic field, an effective gauge flux, whose sign determines the handedness of the spin texture and its underlying magnetic topology.

Because this gauge flux couples directly to charge transport, the ability to create, manipulate, and ultimately switch spin chirality has become a central goal in condensed matter physics and chiral spintronics. Despite its fundamental importance, however, a major open challenge remains: how to electrically reverse topological spin chirality between its two time-reversed states in a controlled and energy-efficient manner. This unresolved question motivates the present work.

Two-dimensional (2D) magnetic van der Waals (vdW) materials³⁻⁸ have rapidly emerged as a fertile platform for exploring unconventional magnetism and topology. Among them, $Co_{1/3}TaS_2$ stands out as a new antiferromagnetic metal with unique magnetic topology^{9,10}. It hosts a

topological 3Q non-coplanar state stabilised by 3/4-filled Fermi surface nesting^{9,10}, forming a tetrahedral four-spin lattice that yields the highest skyrmion density known in vdW magnets. Within this lattice, every three-spin plaquette carries a scalar spin chirality of the same sign. As a result, the effective chirality does not cancel. Instead, it remains a robust, uniform gauge flux throughout the long-period crystal, generating a fictitious magnetic field and a pronounced topological Hall effect⁹⁻¹¹. Co intercalation thus generates an atomic-scale spin-chirality platform ideally suited for studying magnetic topology.

Our recent work¹¹ demonstrated that ionic gating can control this chirality by tuning the Fermi level and nesting conditions, successfully reducing or weakening the topological Hall response¹¹. However, such gating cannot reverse the chirality or toggle between its two time-reversed states. This limitation poses a critical open question: can the topological spin chirality in Co_{1/3}TaS₂ be electrically switched back and forth in a controlled manner? Addressing this question is essential for any practical exploitation of spin chirality in chiral spintronics.

Spin-orbit torque (SOT) provides powerful routes for manipulating spin structures using electrical current^{12,13}. In the conventional approach, SOT arises in magnet/heavy-metal heterostructures, where the spin Hall effect in the heavy metal injects a spin current and exerts a torque on the adjacent magnet¹². Such interfacial SOT can switch magnetic states either with the assistance of an in-plane magnetic field¹⁴ or, more recently, without an external magnetic field through engineered symmetry breaking¹⁵.

Beyond this conventional architecture, a distinct and rapidly developing mechanism, intrinsic

self-SOT, has been identified in vdW magnets. Here, the torque originates within the magnet itself, without requiring a separate spin-source layer of heavy metal¹⁶. A prominent example is Fe₃GeTe₂, where the combination of nontrivial geometry, strong Berry curvature, and topological electronic bands produces a giant intrinsic SOT^{16,17}. Additional inversion-symmetry breaking¹⁸ further enhances this effect. Such a SOT effect enables efficient multi-level current switching¹⁹ and even practical 3-terminal SOT-MRAM²⁰. Subsequent studies have confirmed and expanded self-SOT behavior in Fe₃GeTe₂^{21,22}, and in related vdW magnets such as Fe₃GaTe₂²³⁻²⁵ and Fe_{0.5}Co_{0.5}GeTe₂²⁶.

Importantly, Co_{1/3}TaS₂ also possesses a non-centrosymmetric, mirror-symmetry-broken space group and hosts possible topological bands²⁷. These characteristics naturally suggest the presence of intrinsic self-SOT, making Co_{1/3}TaS₂ a compelling candidate for current-driven self-switching of its topological spin chirality without the need for external fields or heavy-metal layers.

In this work, we demonstrate electrical switching of topological spin chirality using the layered antiferromagnet Co_{1/3}TaS₂ as a model system. We first establish the general concept of switching between time-reversal pairs of spin chirality by electrical current and clarify why the topological 3Q state of Co_{1/3}TaS₂ provides the essential ingredients for realising this functionality. Using the conventional architecture of Co_{1/3}TaS₂/Pt heterostructure, we show that the topological spin chirality is indeed switchable through SOT generated by the spin Hall effect of the Pt layer, thereby validating our proposed chirality-switching mechanism.

Building on this foundation, we discover a distinct intrinsic self-SOT within Co_{1/3}TaS₂ itself: its spin chirality can be switched purely by current, without an external magnetic field and with

high energy efficiency. These two complementary pathways, interfacial SOT and intrinsic self-SOT, establish a comprehensive framework for current-driven manipulation of topological spin chirality. Together, we demonstrate that the quantum antiferromagnet Co_{1/3}TaS₂ can be fully controlled by electrical means, opening up new opportunities in chiral spintronics and magnetic topology.

Concept of switching spin chirality: We begin by elaborating on the fundamental idea of electrically switching spin chirality. As illustrated in **Figure 1**, a non-coplanar spin texture, such as the canonical three-spin configuration on a triangular plaquette, carries a finite topological spin chirality, defined as $\chi = \langle S_1 \cdot (S_2 \times S_3) \rangle$, where S_1 , S_2 , and S_3 denote the spins at the vertices of the triangular plaquette^{1,2}. This scalar chirality acts as a measure of the solid angle subtended by the three spins.

When an electron moves in the vicinity of such a non-coplanar texture, it acquires an additional real-space Berry phase, which effectively behaves as a fictitious magnetic field or quantum gauge flux. This quantum gauge flux deflects the electron trajectory and produces an additional Hall contribution, known as the topological Hall effect^{1,2}. In Fig. 1, the handedness of the spin configuration (chirality) is represented by the left-circular arrow, while the up-straight arrow illustrates the associated gauge flux. This intrinsic correspondence between spin chirality and emergent gauge flux forms the foundation for our central idea: current-driven control of the chirality state, i.e., switching between its time-reversal counterparts by electrically manipulating

the underlying spin texture.

Under a time-reversal symmetry operation, all three spins invert their orientations and the scalar spin chirality $\chi = \langle S_1 \cdot (S_2 \times S_3) \rangle$ changes its sign accordingly. This corresponds to switching from one handedness of the non-coplanar texture to its time-reversed counterpart, depicted by the right-circular chirality and the downward emergent gauge flux. Because the fictitious gauge field directly reflects the sign of the real-space Berry phase, it also reverses under time-reversal operation, consistent with how an ordinary magnetic field transforms.

Our focus is on achieving this transformation electrically, i.e., switching between the two chirality states and their opposite gauge fluxes by applying a current. As schematically illustrated in the upper and lower panels of Fig. 1, the goal is to drive the system between the two time-reversal partners of spin chirality using current-induced torque. Achieving such current-driven chirality reversal provides a direct mechanism to control magnetic topology and the associated emergent electrodynamics.

Spin chirality in topological 3Q states of vdW quantum antiferromagnet $Co_{1/3}TaS_2$: To pursue electrical switching of spin chirality, we employ the vdW antiferromagnet $Co_{1/3}TaS_2$ as our model system because its symmetry, topology, and electronic structure align exceptionally well with the requirement for current-driven control. As shown in **Figure 2a**, $Co_{1/3}TaS_2$ crystallises in a hexagonal, non-centrosymmetric structure with space group $P6_322^9$. Intercalation of Co atoms into the vdW gap of TaS_2 lowers the original centrosymmetric space group $P6_3/mmc$ of pristine 2H-

TaS₂ to this non-centrosymmetric one, simultaneously removing all mirror symmetries⁹.

The combined breaking of inversion and mirror symmetries is crucial, as it enables the generation of current-driven SOT within the material. Such SOTs enable manipulation and switching of the underlying spin texture- either with an in-plane magnetic field^{14,28} or, in suitably engineered systems, even without a magnetic field^{29,30}. These symmetry conditions make Co_{1/3}TaS₂ an ideal candidate for realising electrical control of topological spin chirality as a quantum antiferromagnet.

Moreover, the non-symmorphic symmetry of 6_3 screw symmetry in Co_{1/3}TaS₂ enlarges the primitive unit cell and consequently induces Brillouin zone folding. This zone folding forces electronic bands to intersect or hybridise, particularly along high-symmetry directions, thereby increasing the likelihood of band crossings and symmetry-protected degeneracies. As suggested in previous work²⁷, these band crossings provide natural conditions for generating topological electronic states accompanied by substantial Berry curvature hotspots.

When combined with the material's non-centrosymmetric crystal geometry, this topological electronic structure creates an ideal environment for intrinsic self-SOT, analogous to that observed in vdW ferromagnet Fe₃GeTe₂ and its related compounds¹⁶⁻²⁶. In this picture, the Berry curvature acts as an internal source of spin current, enabling current-driven torque without relying on an external heavy-metal layer. Thus, the symmetry-enforced band topology of Co_{1/3}TaS₂ provides a natural pathway for realising a novel intrinsic self-SOT mechanism capable of manipulating its topological spin chirality.

Beyond its favorable symmetry and electronic characteristics for current-driven SOT, intercalation of Co atoms also gives rise to an exotic non-coplanar spin texture in the layered antiferromagnetic state of Co_{1/3}TaS₂. As shown in Figure 2b, the system hosts a topological tetrahedral 3Q state, stabilised by its 3/4-filled Fermi surface nesting⁹⁻¹¹. The resulting four-spin lattice is composed of two triangular cells, each carrying a scalar spin chirality of the same sign and therefore generating an emergent gauge flux in the same direction, illustrated by the left-circular and up-straight arrows. Consequently, the minimum four-spin unit already exhibits a finite spin chirality, and this nonzero chirality persists throughout the long-period crystal. This microscopic mechanism underlies the pronounced topological Hall effect observed in Co_{1/3}TaS₂⁹⁻¹¹.

Figure 2c presents the two possible 3Q spin configurations: one with positive spin chirality and another with its time-reversal partner bearing negative spin chirality. These two states can be interconverted by applying an out-of-plane magnetic field H_z , which reverses the emergent gauge flux and produces the characteristic Hall hysteresis loop shown in Figure 2d. This pair of chirality states provides the essential two-level system that we seek to switch electrically using current-driven torques.

Therefore, Co intercalation simultaneously engineers the crystal symmetry, electronic topology, and topological spin texture of Co_{1/3}TaS₂, producing a non-centrosymmetric structure, Berry curvature-rich bands, and a robust 3Q chirality lattice. These combined consequences uniquely position Co_{1/3}TaS₂ as an ideal platform to realise our central concept of "current-

switching spin chirality".

Spin chirality switching in Co_{1/3}TaS₂/Pt heterostructure: We first experimentally test the concept of current-driven spin chirality switching using the conventional SOT architecture. Before exploring intrinsic self-SOT, we employ a well-established heterostructure, Co_{1/3}TaS₂ coupled to a heavy metal Pt layer, to verify whether the proposed chirality-switching mechanism can be realised in practice.

Figure 3a illustrates our Co_{1/3}TaS₂/Pt nanodevice. These Co_{1/3}TaS₂ flakes are mechanically exfoliated onto a SiO₂/Si wafer, picked up, and then dropped onto a pre-patterned Pt layer on a SiO₂/Si substrate. Because Pt possesses both high conductivity and a strong spin Hall effect, the applied charge current flows predominantly through the Pt layer and generates an in-plane spin-polarised current. This spin current is injected into Co_{1/3}TaS₂ and exerts an SOT capable of modifying its spin texture.

Figure 3b presents the optical image of the device and the measurement scheme. A large writing current is first applied to induce SOT-mediated switching of the spin chirality. After the writing pulse is removed, a small reading current is used to measure the Hall resistance R_{xy} , which reflects the nonvolatile chiral state established by the preceding pulse. To enable deterministic spin switching, an in-plane magnetic field is applied to break the remaining mirror symmetry parallel to the current direction in Pt, as required in conventional SOT switching^{14,28}.

Figure 3c shows the temperature-dependent longitudinal resistivity (ρ_{xx} -T), exhibiting

metallic behaviour throughout the measured range. The transverse resistivity (ρ_{xy} - H_z) curves in Fig. 3d reveal the characteristic topological Hall effect of Co_{1/3}TaS₂, which appears below the Neel temperature $T_N \sim 25$ K. These measurements confirm that the transferred flakes preserve the intrinsic topological 3Q state and its finite spin chirality.

Crucially, nonvolatile electrical switching of this chirality is demonstrated in Figure 3e. Under a positive in-plane magnetic field H_x =+12 T, the Hall resistance exhibits a clear current-induced hysteresis: applying writing current pulses toggles R_{xy} between two stable values corresponding to opposite chirality states. This unambiguously shows that the current-driven SOT can reverse the topological spin chirality in the Co_{1/3}TaS₂/Pt heterostructure.

Furthermore, reversing the in-plane magnetic field direction inverts the switching polarity (Figure 3f): the same writing current now drives the chirality into the opposite state. This field-polarity dependence mirrors the behavior of SOT-driven magnetization switching in conventional ferromagnet/heavy-metal systems, confirming that an analogous torque mechanism is at work here. Together, these results provide direct experimental validation of our central concept: current-controlled switching of topological spin chirality in the unique quantum magnet Co_{1/3}TaS₂.

Spin chirality self-switching in $Co_{1/3}TaS_2$ itself: We now investigate whether the spin chirality of $Co_{1/3}TaS_2$ can be switched through a distinct intrinsic mechanism, a self-SOT generated within the material itself. As discussed above, Co intercalation gives rise to a unique combination of non-centrosymmetric crystal geometry, band topology, and strong Berry curvature, alongside its

topological 3Q magnetism. These ingredients together favour the emergence of intrinsic self-SOT, analogous to the giant self-SOT discovered in vdW magnet Fe₃GeTe₂¹⁶⁻¹⁸. Furthermore, the reduced symmetry and the absence of mirror planes in Co_{1/3}TaS₂ create conditions that allow magnetic-field-free switching, similar to the symmetry-enabled SOT reversal demonstrated in WTe₂²⁹.

To test this possibility, we perform the same chirality-switching experiment used for the $Co_{1/3}TaS_2/Pt$ case, but with two critical modifications: (1) no Pt layers, ensuring that any torque originates solely from $Co_{1/3}TaS_2$ itself, and (2) no magnetic field, so that any observed switching reflects purely intrinsic symmetry-driven self-SOT. This new configuration enables us to directly investigate whether $Co_{1/3}TaS_2$ can automatically generate sufficient spin-orbit torque to self-switch its topological spin chirality.

Figure 4a shows the optical image of our Co_{1/3}TaS₂ device fabricated without a Pt layer, and Figure 4b displays its temperature-dependent longitudinal resistivity (ρ_{xx} -T), confirming metallic behaviour. The ρ_{xy} - H_z curves in Figure 4c exhibit a clear topological Hall hysteresis below the Neel temperature $T_N \sim 25$ K, demonstrating that the exfoliated flakes retain the intrinsic 3Q chiral antiferromagnetic state.

Crucially, when we apply writing current pulses, the Hall resistance shows a robust current-induced hysteresis (Fig. 4d), indicating that the spin chirality of Co_{1/3}TaS₂ is switched purely by intrinsic self-SOT, without the need for a heavy-metal layer or external magnetic field. Figure 4e summarises magnetic-field-free switching at different temperatures. The Hall resistance switching

is reproduced and observed only below T_N , and vanishes near or above T_N , confirming that the effect originates from spin texture modification and chirality reversal, rather than extrinsic artifacts.

The critical switching current density is approximately 1.8×10⁶ A/cm², comparable to or even lower than values reported in recent highly efficient SOT works^{29,31}. These results therefore establish that Co_{1/3}TaS₂ can autonomously generate sufficient SOT to switch its topological spin chirality, achieving field-free and energy-efficient operation. This self-SOT pathway offers a fundamentally new mechanism for controlling magnetic topology in vdW antiferromagnets.

Conclusion: In summary, we have introduced and experimentally demonstrated the concept of current-switching topological spin chirality using the vdW quantum antiferromagnet Co_{1/3}TaS₂. Taking full advantage of the material's topological 3Q states and its atomic-scale chirality lattice, we first realised chirality reversal through conventional spin-orbit torque in Co_{1/3}TaS₂ /Pt nanodevices, driven by the spin Hall effect of the Pt layer. Building on this foundation, we further identified and exploited a distinct intrinsic self-SOT, enabling field-free and heavy-metal-free electrical switching of spin chirality within Co_{1/3}TaS₂ itself.

These complementary approaches, both classic and unconventional SOT, collectively establish a comprehensive framework for electrically creating, controlling, and manipulating topological spin chirality. Our findings reveal a new dimension of chiral spintronics and provide a versatile strategy that can be applied to other skyrmion systems, non-coplanar magnets, and chirality-related quantum effects.

Experimental Section

Single crystal synthesis: Co_{1/3}TaS₂ single crystals were grown by a two-step growth method. To ensure compositional homogeneity, a precursor was prepared via a solid-state reaction. A well-ground mixture of Co (Alfa Aesar, >99.99%), Ta (Sigma Aldrich, >99.99%), and S (Sigma Aldrich, >99.99%) was sealed in an evacuated quartz ampoule and sintered at 900 °C for 10 days. The resulting polycrystalline precursor and I₂ transport agent (4.5 mg I₂/cm³) were then placed in an evacuated quartz tube, and single crystals were grown by the chemical vapor transport (CVT) method. The quartz tube was heated in a two-zone furnace with a temperature gradient from 960°C to 840 °C for 2 weeks. The obtained single crystals were characterised by X-ray diffraction (XRD) and Raman spectroscopy, as shown in Figures S1 and S2.

Device fabrication: Co_{1/3}TaS₂ nanoflakes were mechanically exfoliated onto a SiO₂/Si wafer, and a suitable sample was chosen for transport investigations. The polymethyl methacrylate (PMMA) A7 was spin-coated onto the nanoflake at a rate of 4000 rpm, and then post-baked at a mild temperature of 130 °C for 1.5 mins. Afterwards, the electrodes were designed using the electron beam lithography, and then 80/10 nm Au/Ti metals were deposited in order by the electron beam evaporator. For the Co_{1/3}TaS₂/Pt heterostructure, a Pt layer was first pre-patterned onto a bare SiO₂/Si substrate, and the chosen Co_{1/3}TaS₂ nanoflake was picked up and then dropped down onto the Pt layer by the PCL transfer technique³²⁻³⁴.

Electrical Transport measurement: Electrical transport measurements were performed using a home-built closed-circulation-resistance setup, as well as a commercial cryogenic system. Those measurements were carried out using a Keithley 6220, a Keithley 2182, and a lock-in amplifier. The ρ_{xy} - H_z curves were measured with an applied out-of-plane magnetic field.

Acknowledgments

K.-X.Z. and S.L. contributed equally to this work. We acknowledge Jihoon Keum for the helpful discussions and experimental support. The work at CQM and SNU was supported by the Samsung Science & Technology Foundation (Grant No. SSTF-BA2101-05) and the Leading Researcher Program of the National Research Foundation of Korea (Grant No. RS-2020-NR049405).

References

- 1. Nagaosa, N., Sinova, J., Onoda, S., MacDonald, A. H. & Ong, N. P. Anomalous Hall effect. *Rev. Mod. Phys.* **82**, 1539-1592 (2010).
- 2. Petrović, A. P., Psaroudaki, C., Fischer, P., Garst, M. & Panagopoulos, C. Colloquium: Quantum properties and functionalities of magnetic skyrmions. *Rev. Mod. Phys.* **97**, 031001 (2025).
- 3. Park, J. G. Opportunities and challenges of 2D magnetic van der Waals materials: magnetic graphene? *J. Phys. Condens. Matter* **28**, 301001 (2016).
- 4. Lee, J. U., Lee, S., Ryoo, J. H., Kang, S., Kim, T. Y., Kim, P., Park, C. H., Park, J. G. & Cheong, H. Ising-Type Magnetic Ordering in Atomically Thin FePS₃. *Nano Lett.* **16**, 7433-7438 (2016).
- 5. Huang, B., Clark, G., Navarro-Moratalla, E., Klein, D. R., Cheng, R., Seyler, K. L., Zhong, D., Schmidgall, E., McGuire, M. A., Cobden, D. H., Yao, W., Xiao, D., Jarillo-Herrero, P. & Xu, X. Layer-dependent ferromagnetism in a van der Waals crystal down to the monolayer limit. *Nature* **546**, 270-273 (2017).
- 6. Gong, C., Li, L., Li, Z., Ji, H., Stern, A., Xia, Y., Cao, T., Bao, W., Wang, C., Wang, Y., Qiu, Z. Q., Cava, R. J., Louie, S. G., Xia, J. & Zhang, X. Discovery of intrinsic ferromagnetism in two-dimensional van der Waals crystals. *Nature* **546**, 265-269 (2017).
- 7. Burch, K. S., Mandrus, D. & Park, J. G. Magnetism in two-dimensional van der Waals materials. *Nature* **563**, 47-52 (2018).
- 8. Zhang, K.-X., Park, G., Lee, Y., Kim, B. H. & Park, J.-G. Magnetoelectric effect in van der Waals magnets. *npj Quantum Mater.* **10**, 6 (2025).
- 9. Park, P., Cho, W., Kim, C., An, Y., Kang, Y. G., Avdeev, M., Sibille, R., Iida, K., Kajimoto, R., Lee, K. H., Ju, W., Cho, E. J., Noh, H. J., Han, M. J., Zhang, S. S., Batista, C. D. & Park, J. G. Tetrahedral triple-Q magnetic ordering and large spontaneous Hall conductivity in the metallic triangular antiferromagnet Co_{1/3}TaS₂. *Nat. Commun.* **14**, 8346 (2023).
- 10. Takagi, H., Takagi, R., Minami, S., Nomoto, T., Ohishi, K., Suzuki, M. T., Yanagi, Y., Hirayama, M., Khanh, N. D., Karube, K., Saito, H., Hashizume, D., Kiyanagi, R., Tokura, Y., Arita, R., Nakajima, T. & Seki, S. Spontaneous topological Hall effect induced by non-coplanar antiferromagnetic order in intercalated van der Waals materials. *Nat. Phys.* 19, 961-968 (2023).
- 11. Kim, J., Zhang, K. X., Park, P., Cho, W., Kim, H., Noh, H. J. & Park, J. G. Electrical control of topological 3Q state in intercalated van der Waals antiferromagnet Co_x-TaS₂. *Nat. Commun.* **16**, 8943 (2025).
- 12. Kurebayashi, H., Garcia, J. H., Khan, S., Sinova, J. & Roche, S. Magnetism, symmetry and spin transport in van der Waals layered systems. *Nat. Rev. Phys.* **4**, 150-166 (2022).
- 13. Zhang, K.-X., Cheon, S., Kim, H., Park, P., An, Y., Son, S., Cui, J., Keum, J., Choi, J., Jo, Y., Ju, H., Lee, J. S., Lee, Y., Avdeev, M., Kleibert, A., Lee, H.-W. & Park, J.-G. Current-driven collective control of helical spin texture in van der Waals antiferromagnet. *Phys.*

- Rev. Lett. 134, 176701 (2025).
- 14. Miron, I. M., Garello, K., Gaudin, G., Zermatten, P. J., Costache, M. V., Auffret, S., Bandiera, S., Rodmacq, B., Schuhl, A. & Gambardella, P. Perpendicular switching of a single ferromagnetic layer induced by in-plane current injection. *Nature* **476**, 189-193 (2011).
- 15. Yu, G., Upadhyaya, P., Fan, Y., Alzate, J. G., Jiang, W., Wong, K. L., Takei, S., Bender, S. A., Chang, L. T., Jiang, Y., Lang, M., Tang, J., Wang, Y., Tserkovnyak, Y., Amiri, P. K. & Wang, K. L. Switching of perpendicular magnetization by spin-orbit torques in the absence of external magnetic fields. *Nat. Nanotechnol.* **9**, 548-554 (2014).
- 16. Zhang, K., Han, S., Lee, Y., Coak, M. J., Kim, J., Hwang, I., Son, S., Shin, J., Lim, M., Jo, D., Kim, K., Kim, D., Lee, H.-W. & Park, J.-G. Gigantic current control of coercive field and magnetic memory based on nm-thin ferromagnetic van der Waals Fe₃GeTe₂. *Adv. Mater.* 33, 2004110 (2021).
- 17. Johansen, Ø., Risinggård, V., Sudbø, A., Linder, J. & Brataas, A. Current Control of Magnetism in Two-Dimensional Fe₃GeTe₂. *Phys. Rev. Lett.* **122**, 217203 (2019).
- 18. Zhang, K.-X., Ju, H., Kim, H., Cui, J., Keum, J., Park, J.-G. & Lee, J. S. Broken inversion symmetry in van der Waals topological ferromagnetic metal iron germanium telluride. *Adv. Mater.* **36**, 2312824 (2024).
- 19. Zhang, K., Lee, Y., Coak, M. J., Kim, J., Son, S., Hwang, I., Ko, D. S., Oh, Y., Jeon, I., Kim, D., Zeng, C., Lee, H.-W. & Park, J.-G. Highly efficient nonvolatile magnetization switching and multi-level states by current in single van der Waals topological ferromagnet Fe₃GeTe₂. *Adv. Funct. Mater.* **31**, 2105992 (2021).
- 20. Cui, J., Zhang, K.-X. & Park, J.-G. All van der Waals Three-Terminal SOT-MRAM Realized by Topological Ferromagnet Fe₃GeTe₂. *Adv. Electron. Mater.* **10**, 2400041 (2024).
- 21. Martin, F., Lee, K., Schmitt, M., Liedtke, A., Shahee, A., Simensen, H. T., Scholz, T., Saunderson, T. G., Go, D., Gradhand, M., Mokrousov, Y., Denneulin, T., Kovács, A., Lotsch, B., Brataas, A. & Kläui, M. Strong bulk spin-orbit torques quantified in the van der Waals ferromagnet Fe₃GeTe₂. *Mater. Res. Lett.* **11**, 84-89 (2022).
- 22. Robertson, I. O., Tan, C., Scholten, S. C., Healey, A. J., Abrahams, G. J., Zheng, G., Manchon, A., Wang, L. & Tetienne, J.-P. Imaging current control of magnetization in Fe₃GeTe₂ with a widefield nitrogen-vacancy microscope. *2D Mater.* **10**, 015023 (2022).
- 23. Deng, Y., Wang, M., Xiang, Z., Zhu, K., Hu, T., Lu, L., Wang, Y., Ma, Y., Lei, B. & Chen, X. Room-Temperature Highly Efficient Nonvolatile Magnetization Switching by Current in van der Waals Fe₃GaTe₂ Devices. *Nano Lett.* **24**, 9302-9310 (2024).
- 24. Zhang, G., Wu, H., Yang, L., Jin, W., Xiao, B., Zhang, W. & Chang, H. Room-temperature Highly-Tunable Coercivity and Highly-Efficient Multi-States Magnetization Switching by Small Current in Single 2D Ferromagnet Fe₃GaTe₂. *ACS Mater. Lett.* **6**, 482-488 (2024).
- 25. Yan, S., Tian, S., Fu, Y., Meng, F., Li, Z., Lei, H., Wang, S. & Zhang, X. Highly Efficient Room-Temperature Nonvolatile Magnetic Switching by Current in Fe₃GaTe₂ Thin Flakes. *Small* **20**, 2311430 (2024).

- Zhang, H., Chen, X., Wang, T., Huang, X., Chen, X., Shao, Y. T., Meng, F., Meisenheimer, P., N'Diaye, A., Klewe, C., Shafer, P., Pan, H., Jia, Y., Crommie, M. F., Martin, L. W., Yao, J., Qiu, Z., Muller, D. A., Birgeneau, R. J. & Ramesh, R. Room-Temperature, Current-Induced Magnetization Self-Switching in A Van Der Waals Ferromagnet. *Adv. Mater.* 36, 2308555 (2024).
- 27. Park, P., Kang, Y. G., Kim, J., Lee, K. H., Noh, H. J., Han, M. J. & Park, J. G. Field-tunable toroidal moment and anomalous Hall effect in noncollinear antiferromagnetic Weyl semimetal Co_{1/3}TaS₂. *npj Quantum Mater.* 7, 42 (2022).
- 28. Wang, X., Tang, J., Xia, X., He, C., Zhang, J., Liu, Y., Wan, C., Fang, C., Guo, C., Yang, W., Guang, Y., Zhang, X., Xu, H., Wei, J., Liao, M., Lu, X., Feng, J., Li, X., Peng, Y., Wei, H., Yang, R., Shi, D., Zhang, X., Han, Z., Zhang, Z., Zhang, G., Yu, G. & Han, X. Current-driven magnetization switching in a van der Waals ferromagnet Fe₃GeTe₂. *Sci. Adv.* 5, eaaw8904 (2019).
- Kao, I. H., Muzzio, R., Zhang, H., Zhu, M., Gobbo, J., Yuan, S., Weber, D., Rao, R., Li, J., Edgar, J. H., Goldberger, J. E., Yan, J., Mandrus, D. G., Hwang, J., Cheng, R., Katoch, J. & Singh, S. Deterministic switching of a perpendicularly polarized magnet using unconventional spin-orbit torques in WTe₂. *Nat. Mater.* 21, 1029-1034 (2022).
- 30. Keum, J., Zhang, K.-X., Cheon, S., Kim, H., Cui, J., Park, G., Chang, Y., Kim, M., Lee, H.-W. & Park, J.-G. Novel magnetic-field-free switching behavior in vdW-magnet/oxide heterostructure. *Adv. Mater.* **37**, 2412037 (2025).
- 31. Wang, F., Shi, G., Kim, K. W., Park, H. J., Jang, J. G., Tan, H. R., Lin, M., Liu, Y., Kim, T., Yang, D., Zhao, S., Lee, K., Yang, S., Soumyanarayanan, A., Lee, K. J. & Yang, H. Field-free switching of perpendicular magnetization by two-dimensional PtTe₂/WTe₂ van der Waals heterostructures with high spin Hall conductivity. *Nat. Mater.* 23, 768-774 (2024).
- 32. Son, S., Shin, Y. J., Zhang, K., Shin, J., Lee, S., Idzuchi, H., Coak, M. J., Kim, H., Kim, J., Kim, J. H., Kim, M., Kim, D., Kim, P. & Park, J.-G. Strongly adhesive dry transfer technique for van der Waals heterostructure. *2D Mater.* 7, 041005 (2020).
- 33. Kim, J., Son, S., Coak, M. J., Hwang, I., Lee, Y., Zhang, K. & Park, J.-G. Observation of plateau-like magnetoresistance in twisted Fe₃GeTe₂/Fe₃GeTe₂ junction. *J. Appl. Phys.* **128**, 093901 (2020).
- 34. Park, G., Son, S., Kim, J., Chang, Y., Zhang, K., Kim, M., Lee, J. & Park, J.-G. New twisted van der Waals fabrication method based on strongly adhesive polymer. *2D Mater.* **11**, 025021 (2024).

Figures

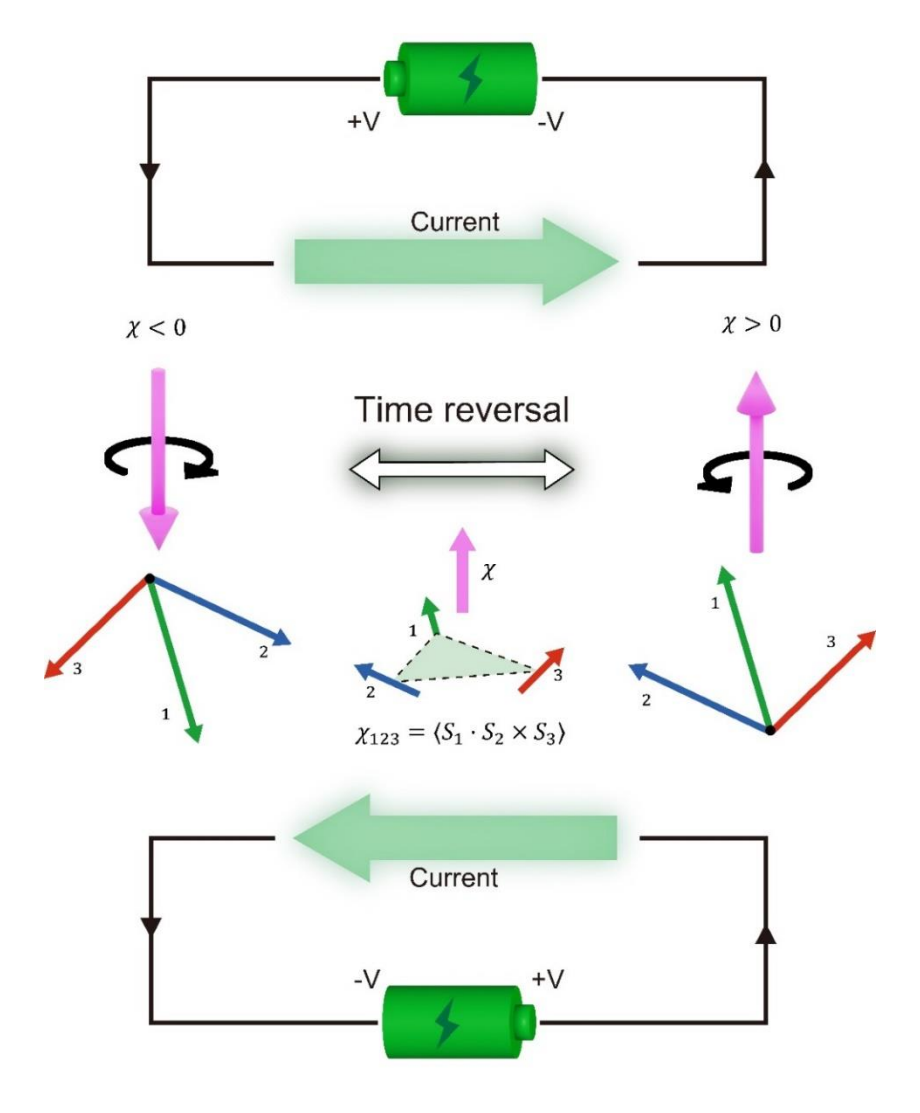


Figure 1. Concept of current-switching spin chirality and its associated gauge flux. In a non-coplanar three-spin configuration, spin chirality can arise as $\chi = \langle S_1 \cdot (S_2 \times S_3) \rangle$, where S_1 , S_2 , and S_3 represent spins at the vertices of a triangular plaquette. It can give rise to a real-space Berry phase to the electron's wave function and behaves like a fictitious magnetic field or gauge flux, generating the topological Hall effect. As illustrated, the spin texture determines both the chirality of spin and the direction of the gauge flux. Under a time-reversal operation, spin, chirality,

and gauge flux all flip their directions simultaneously. For fundamental control and practical application, we propose the idea of switching spin chirality by current, as highlighted in the thick green arrows.

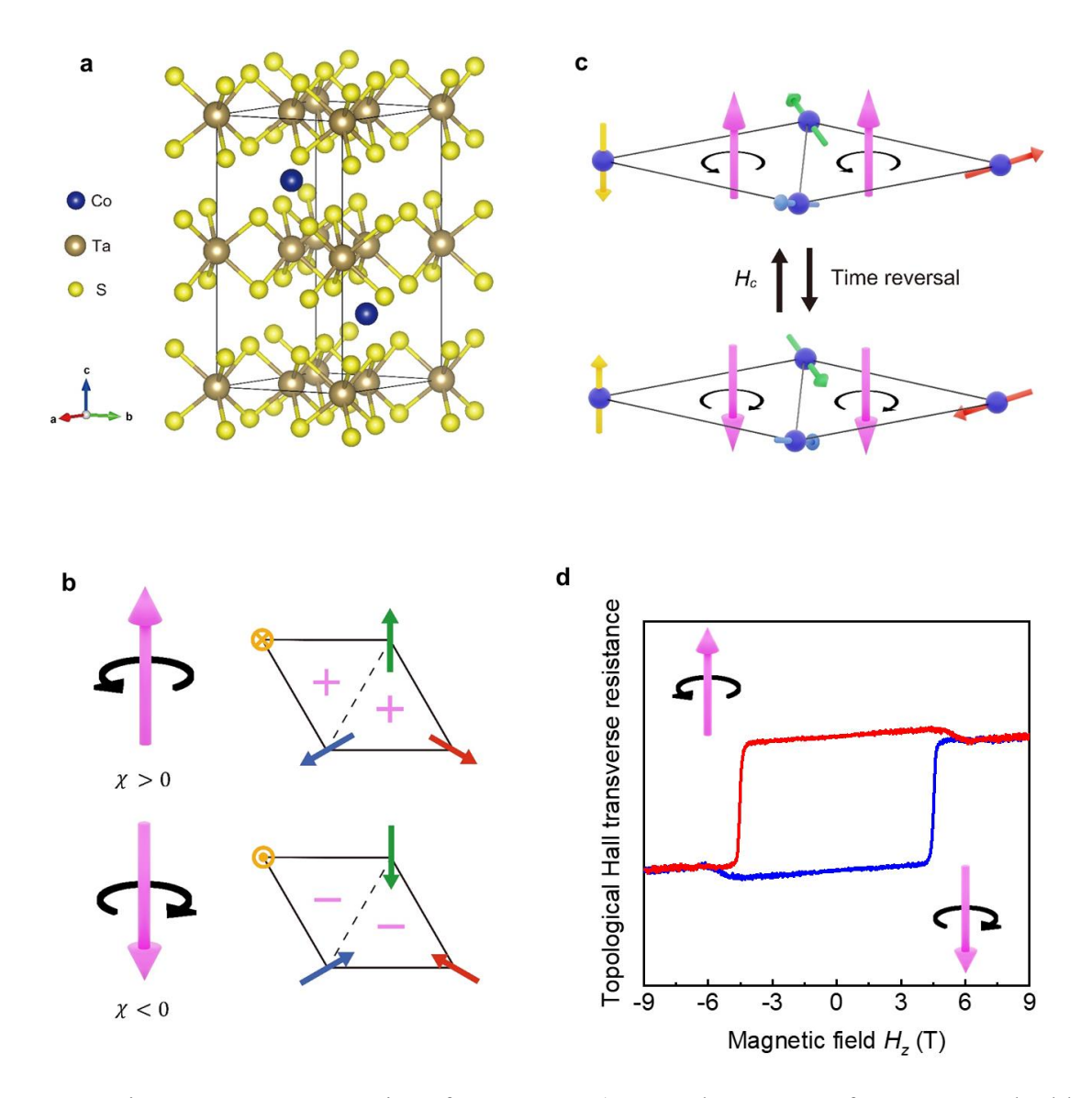


Figure 2. Unique quantum properties of $Co_{1/3}TaS_2$. a) Crystal structure of $Co_{1/3}TaS_2$. The black line indicates a unit cell, and the blue, brown, and yellow balls represent Co, Ta, and S atoms, respectively. Co atoms are intercalated into the vdW gap of the TaS_2 layer, making several

important quantum consequences as numerated in the main text. b) Spin chirality of the topological tetrahedral 3Q states in $Co_{1/3}TaS_2$. For the four-spin primitive lattice, each three-spin cell hosts a spin chirality of the same sign, rendering a robust, nonzero spin chirality throughout the whole crystal structure. c) Under time-reversal symmetry operation, e.g., by out-of-plane magnetic field H_z , each spin flips in the four-spin lattice, so do the spin chirality and gauge flux. d) Experimental outcome of (c): hysteresis loop of the topological Hall effect by sweeping H_z .

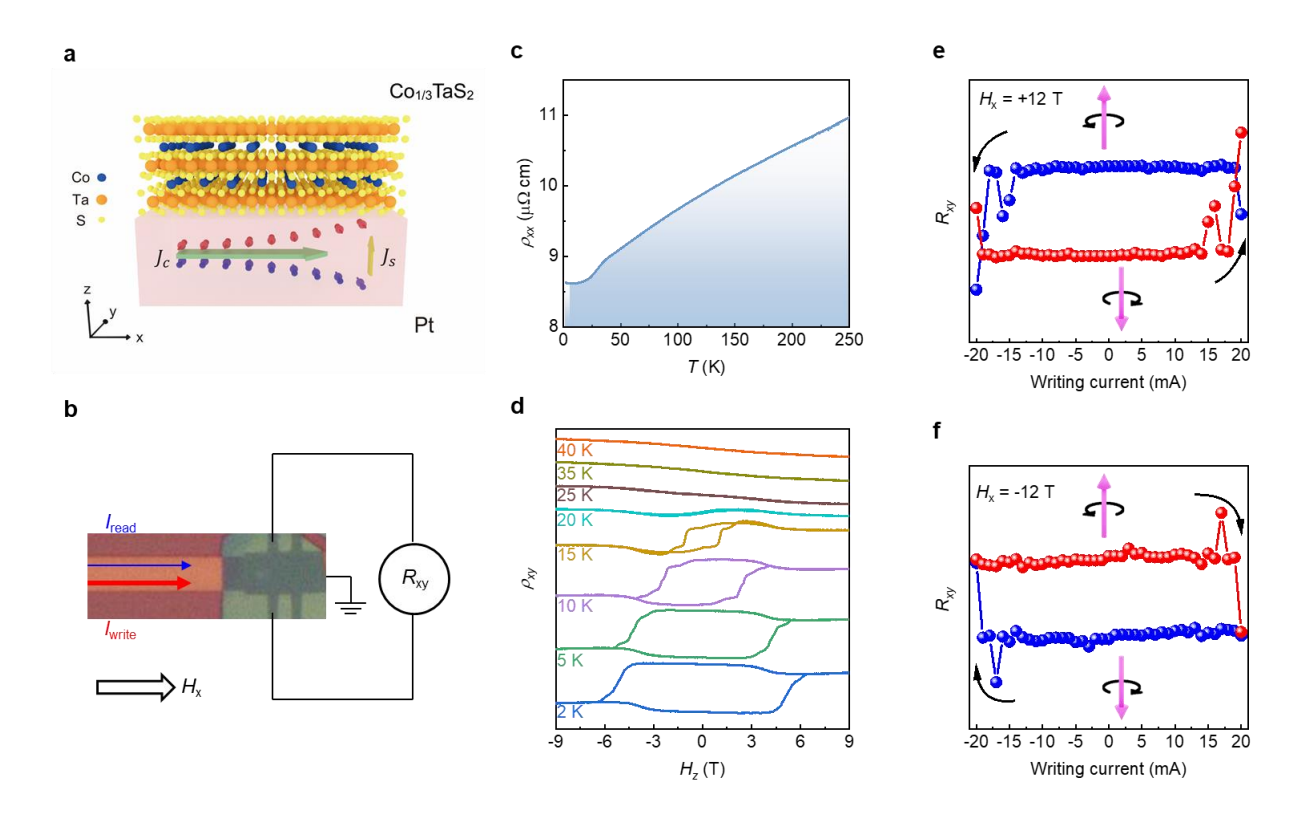


Figure 3. Electrical switching of spin chirality by current-driven SOT in $Co_{1/3}TaS_2/Pt$ heterostructure. a) Schematic of the $Co_{1/3}TaS_2/Pt$ device and spin Hall effect of the Pt layer. Charge current generates a spin current of in-plane spin polarisation, injecting into $Co_{1/3}TaS_2$ and introducing the spin-orbit torque effect on $Co_{1/3}TaS_2$'s spin texture. b) Real device and switching

measurement schematic. The writing current I_{write} is first applied, then turned off. Afterwards, a small reading current I_{read} of 100 μ A is applied to read out the transverse resistance R_{xy} . c) ρ_{xx} -T curve of the device, showing a metallic behavior. d) ρ_{xy} - H_z curves at various temperatures, where clear hysteresis loops emerge below the Neel temperature of T_N -25 K. e) R_{xy} switching by sweeping the writing current under H_x =+12 T. The spin chirality switching by current is achieved, as indicated by the circular and straight arrows. f) Spin chirality switching by current with H_x =-12 T, where the switching polarity changes.

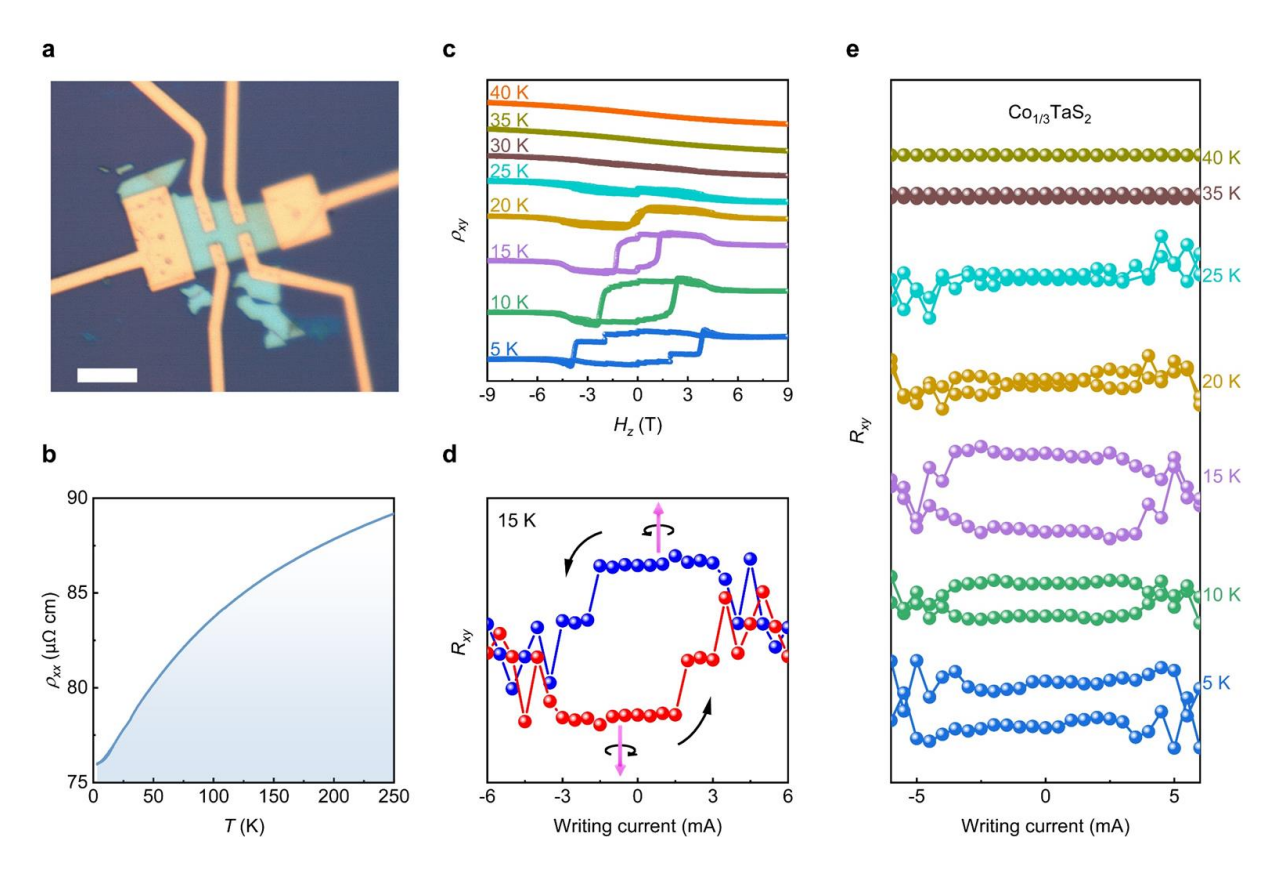


Figure 4. Current switching spin chirality by intrinsic self-SOT in $Co_{1/3}TaS_2$ itself. a) Optical image of our pristine $Co_{1/3}TaS_2$ device. The white scale bar is 10 μ m. b) ρ_{xx} -T curve of the device,

showing a metallic behavior. c) ρ_{xy} - H_z curves at various temperatures, where clear hysteresis loops emerge below the Neel temperature of T_N ~25 K. d) Sin chirality switching by current in pristine $Co_{1/3}TaS_2$ alone. e) Current-driven spin chirality switching emerges below the Neel temperature of T_N ~25 K, and disappears near or above T_N , pointing to its magnetism origin and SOT scenario.